11-1-2018

Hemodynamic Characteristics of Stable and Unstable Vertebrobasilar Dolichoectatic and Fusiform Aneurysms

Waleed Brinjikji
Mayo Clinic Rochester, MN

Bong Jae Chung
Montclair State University, chungb@mail.montclair.edu

Ding Yong-Hong
AP-HP Assistance Publique - Hopitaux de Paris

John T. Wald
Mayo Clinic Rochester, MN

Fernando Mut
George Mason University

See next page for additional authors

ORIGINAL RESEARCH

Hemodynamic characteristics of stable and unstable vertebrobasilar dolichoectatic and fusiform aneurysms

Waleed Brinjikji,[1,2] Bongjae Chung,[3] Ding Yong-Hong,[1] John T Wald,[1] Fernando Mut,[3] Ramanathan Kadirvel,[1] David F Kallmes,[1,2] Aymeric Rouchaud,[4] Giuseppe Lanzino,[1,2] Juan R Cebral[3]

[1]Department of Radiology, Mayo Clinic, Rochester, Minnesota, USA
[2]Department of Neurosurgery, Mayo Clinic, Rochester, Minnesota, USA
[3]Department of Bioengineering, Volgenau School of Engineering, George Mason University, Fairfax, Virginia, USA
[4]Department of Interventional Neuroradiology, Bicetre Hospital, Paris, France

Correspondence to
Dr Waleed Brinjikji, Department of Radiology, Mayo Clinic, Rochester, MN559005, USA; brinjikji.waleed@gmail.com

Received 8 January 2018
Revised 20 February 2018
Accepted 21 February 2018
Published Online First 16 March 2018

ABSTRACT

Background and purpose Vertebrobasilar dolichoectatic and fusiform aneurysms (VBDAs) are known to have a poor natural history, with high rates of growth, rupture, and stroke. The purpose of this study was to identify hemodynamic characteristics that differ between VBDAs associated with growth, rupture, and stroke.

Materials and methods VBDAs with CT angiography or MR angiography followed longitudinally without treatment were studied. Unstable aneurysms were defined as those that grew or ruptured during follow-up. Aneurysms associated with stroke were defined as those associated with posterior circulation infarct at follow-up. Baseline data, including demographics, comorbidities, and aneurysm morphology and size were collected. Image based computational fluid dynamics models were created and run under pulsatile flow conditions. Relevant hemodynamic and geometric variables were calculated and compared between groups (stable vs unstable and no stroke vs stroke) using the Wilcoxon test.

Results A total of 37 VBDAs were included (24 stable, 13 unstable; 30 no stroke, 7 stroke). Unstable aneurysms had lower shear rates (P=0.05), blood flow velocity (P=0.03), and lower vorticity (P=0.049) than stable aneurysms. In addition, unstable aneurysms had higher mean oscillatory shear indices (P=0.001). There were no differences in the hemodynamic characteristics of aneurysms in the stroke group compared with the non-stroke group.

Conclusion This small study suggests there may be hemodynamic differences between unstable and stable VBDAs. Unstable VBDAs appear to be under lower flow conditions with lower velocity, vorticity, and shear rates, and have more oscillatory flow. There was no difference in the hemodynamic characteristics of aneurysms in the stroke and no stroke group.

INTRODUCTION

Longitudinal and cross sectional studies of patients with vertebrobasilar dolichoectatic and fusiform aneurysms (VBDAs) have found that these lesions are associated with a very poor natural history, with high rates of aneurysm growth (up to 6%/year), rupture (up to 2%/year), and stroke.[1–6] Identifying variables associated with instability of VBDAs and subsequent acute ischemic stroke is important as the morbidity associated with surgical and endovascular treatment of these lesions is high.[1–6] A number of studies have found that aneurysm size and morphology are the primary predictors of aneurysm instability and risk of aneurysm associated ischemia, as larger aneurysms and aneurysms with fusiform and transitional morphologies have been shown to be more high risk.[1–6] Clinical variables associated with VBDA instability and associated stroke include patient smoking history, increasing patient age, and hypertension.[5 6]

While clinical and angiographic risk factors for VBDA instability are increasingly well established, it is reasonable to assume that intra-aneurysmal hemodynamics plays a significant role in aneurysm natural history. Computational fluid dynamic models in saccular aneurysms suggest an association between aneurysm hemodynamics and aneurysm growth and rupture.[7–9] However, to date, there have been no studies examining the association between aneurysm hemodynamics and the natural history of VBDAs. Developing an understanding of the hemodynamic characteristics of unstable VBDAs may be helpful in identifying mechanisms associated with aneurysm growth and rupture beyond size and morphology.

In order to study the role of hemodynamic parameters in the natural history of VBDAs, we performed an exploratory study examining various computational fluid dynamics (CFD) parameters to determine the association between aneurysm hemodynamics and VBDA growth/rupture as well as aneurysm hemodynamics and risk of posterior circulation ischemia associated with VBDAs. We hypothesized that there would be differences in the hemodynamic characteristics between unstable and stable aneurysms as well as aneurysms associated with ischemia.

METHODS

Patient selection

Following institutional review board approval, 37 patients with unruptured VBDAs with serial imaging follow-up at a single site were included in the study. Inclusion criteria were the following: (1) fusiform, non-dissecting aneurysms located along the intradural vertebral artery or basilar artery, (2) at least one baseline CT angiogram or MR angiogram set of images, (3) serial imaging of the aneurysm

To cite: Brinjikji W, Chung B, Yong-Hong D, *et al*. *J NeuroIntervent Surg* 2018;**10**:1102–1107.

with either CT angiography (CTA), MR angiography (MRA), or conventional angiography, and (4) imaging evidence of growth, rupture, or posterior circulation stroke related to the aneurysm on imaging follow-up or documented stability of the aneurysm with serial intracranial vascular imaging with the first and last angiographic images spaced at least 12 months apart and clinical follow-up of at least 1 year. Baseline images were used for analysis. Aneurysms that presented as ruptured and aneurysms that lacked serial imaging were excluded from the study. These aneurysms did not undergo treatment due to the high risks associated with endovascular and surgical treatment of these lesions.

Patient groups and imaging assessment

Two separate analyses were performed: (1) an analysis examining hemodynamic factors associated with aneurysm instability and (2) an analysis examining hemodynamic factors associated with posterior circulation infarct. For the analysis of instability, aneurysm instability was defined as aneurysm growth (defined as an increase in size of 1 mm or more, as determined by two reviewers when evaluating multiplanar reconstruction images of CTA/MRA images) or rupture on follow-up, and patients were divided into two groups: stable and unstable. We assumed that CTA and MRA would yield similar measurements. Mural T1 hyperintensity, indicating intramural hemorrhage, was also collected. For the analysis of posterior circulation infarct, patients were divided into a stroke or no stroke group based on the presence of CT or MRI evidence of new posterior circulation infarct with associated clinical symptoms. All images were interpreted by two neuroradiologists.

Baseline aneurysm related data that were collected included size and morphology (dolichoectatic, fusiform, or transitional, according to the criteria of Flemming[5 6]). Definitions of aneurysm morphology according to the Flemming criteria are as follows: fusiform are 1.5×normal diameter without a definable neck involving a portion of an arterial segment (either vertebral or basilar) with any degree of tortuosity; dolichoectatic have uniform aneurysmal dilatation of any artery >1.5×normal, involving either the entire basilar or vertebral artery, or both, with any degree of tortuosity; and transitional have uniform aneurysmal dilatation of an artery >1.5×normal, involving the vertebral or basilar artery, or both, with a superimposed dilatation of a portion of the involved arterial segment. Aneurysms were also categorized using the Mizutani system. Mizutani type 1 aneurysms were excluded. Mizutani type 2 aneurysms were segmental ectasias with a smooth fusiform contour while Mizutani type 3 aneurysms were those with a tortous fusiform.

Demographic data, including age and gender, were collected. Comorbidities included were coronary artery disease, peripheral artery disease, hypertension, diabetes mellitus, hyperlipidemia, and tobacco use.

Aneurysm hemodynamics modeling

The methods used for aneurysm modeling have been previously described by Cebral *et al*.[10] Patient specific vascular models were constructed from the axial MRA and CTA images of the initial examination. Segmentation was carried out using region growing and deformable models.[10] Region growing algorithms start with a seed voxel within the vessel and recursively mark other connected voxels within a specified intensity range. It is similar to a thresholding approach but it produces a single connected region. A surface model is then reconstructed as an intensity iso-surface, and subsequently deformed (adjusted) under the action of internal elastic forces and external forces from the image intensity gradient. This geometry adjustment step is called a deformable model. Models were smoothed and truncated perpendicularly to the vessel axis, keeping as much of the proximal parent artery as possible to ensure proper representation of secondary swirling flows in the parent artery and aneurysm orifice.[11] Unstructured grids were generated with a minimum resolution of 0.2 mm, resulting in meshes ranging from about 2 to 8 million tetrahedral elements. Blood was approximated as a Newtonian fluid with density $\rho = 1.0\,g/cm^3$ and viscosity $\mu = 0.04$ poise. The incompressible Navier–Stokes equations were numerically solved using inhouse finite elements solver. The flow solver is called FELFO and has been extensively verified and validated in a wide variety of applications and compared against in vivo angiography observations.[12 13] Pulsatile flow boundary conditions were imposed at the model inlet using the Womersley profile. The flow waveform was derived from phase contrast MR measurements in the vertebral artery of normal subjects[14] and scaled with the inlet boundary area.[15] The flow from the parent artery was split among the outlet boundaries according to the principle of minimum work (Murray's law).[16] Wall compliance was neglected and no slip boundary conditions were applied at the walls. Numerical simulations were carried out for two cardiac cycles, and the flow field was saved at 0.01 s intervals during the second cycle for subsequent analysis.

Hemodynamic analysis

Aneurysm inlets were manually delineated on the reconstructed models.[17] A few points on the aneurysm inlet were interactively selected and connected along lines of minimum distance on the surface (geodesic). Next, the aneurysm inlet orifice was triangulated and used to subdivide the computational mesh into two regions corresponding to the aneurysm and the parent artery. The distal end of the aneurysm (outlet) was similarly delineated and used in combination with the inlet to label all the mesh elements within the aneurysm. A number of flow variables defined on the aneurysm region were quantified and used to characterize the aneurysm hemodynamics. Volumetric factors included: mean aneurysm kinetic energy (KE); mean aneurysm velocity (VE); mean aneurysm shear rate (SR) (a measure of the deformation of the fluid elements); mean aneurysm vorticity (VO) (a measure of the rotational velocity of fluid elements); mean aneurysm viscous dissipation (VD); and vortex core line length (CORELEN), which provides a measure of the complexity of the aneurysmal flow structure.[18] Surface factors included mean, maximum, and minimum wall shear stress (WSS, WSSmax, WSSmin) computed over the aneurysm sac; and mean oscillatory shear index (OSI). Additionally, a number of geometric variables were calculated, including aneurysm maximum diameter; aneurysm volume and surface area; and Gaussian and mean curvature. More details and exact definitions of these variables are provided by Mut *et al*.[17]

Statistical analysis

Mean values for hemodynamics and geometric variables were compared across the stable and unstable groups and the stroke and no stroke groups. Non-parametric Wilcoxon rank sum tests were performed to determine the statistical significance of the hemodynamic differences between growing and stable aneurysms. When comparing baseline clinical data, the Student's t test was used for comparison of continuous variables and the χ^2 test was used for comparison of categorical variables. Differences were considered statistically significant if the two tailed P values were <0.05 (95% CI).

Table 1 Baseline characteristics of stable and unstable aneurysms

	Stable	Unstable	P value
No of patients (%)	24 (64.9)	13 (35.1)	–
Age (years) (mean (SD))	60.6 (13.6)	58.8 (15.7)	0.74
Men (n (%))	20 (83.3)	9 (69.2)	0.41
Follow-up (months) (mean (SD))	40.8 (54.1)	51.9 (41.4)	0.52
Aneurysm type (n (%))			
Flemming			
Fusiform	6 (25.0)	4 (30.8)	
Dolichoectatic	13 (54.2)	2 (15.4)	
Transitional	5 (20.8)	7 (53.9)	0.04
Mizutani type			
Type 2	13 (54.2)	2 (15.4)	
Type 3	11 (45.8)	11 (84.6)	0.035
Mural T1 hyperintensity (n (%))	8 (34.8)	8 (61.5)	0.12
Maximum diameter (mm) (mean (SD))	7.6 (1.8)	11.9 (5.0)	0.01
Comorbidities (n (%))			
CAD	6 (25.0)	7 (53.9)	0.08
PAD	0 (0.0)	0 (0.0)	1
Hypertension	16 (66.7)	11 (84.6)	0.24
Diabetes mellitus	2 (8.3)	3 (23.1)	0.21
Hyperlipidemia	14 (58.3)	9 (69.2)	0.51
Tobacco use	3 (12.5)	8 (61.5)	0.002

CAD, coronary artery disease; PAD, peripheral artery disease.

Table 2 Hemodynamic outcomes of stable and unstable aneurysms

	Stable		Unstable		P value
Variable	Mean	SD	Mean	SD	
Hemodynamics					
Kinetic energy (erg)	446.6	453.14	239.11	393.78	0.16
Shear rate (1/s)	153.2	118.91	84.89	87.07	**0.05**
Velocity (cm/s)	15.01	7.74	9.3	6.79	**0.03**
Vorticity (1/s)	219.8	170.65	120.11	122.71	**0.049**
Viscous dissipation (erg)	764.5	1194	353.58	843.99	0.23
WSSmax (dyn/cm^2)	181	177.33	152.68	171.79	0.64
WSSmin (dyn/cm^2)	0.12	0.38	0.01	0.01	0.18
WSSmean (dyn/cm^2)	18.05	14.66	10.82	12.16	0.12
OSImax	0.4	0.11	0.46	0.03	**0.02**
OSImean	0.01	0.01	0.04	0.02	**0.001**
Core line length/flow complexity (cm)	4.32	5.01	11.67	10.53	**0.03**
POD entropy/flow stability	0.11	0.07	0.24	0.11	**0.001**
POD num/flow stability	1	0	1.31	0.63	0.1
Maximum velocity (cm/s)	88.64	75.01	83.52	81.21	0.85
Mean maximum velocity (cm/s)	50.9	42.4	48.8	47.7	0.89
Geometry					
Gaussian curvature	0.02	0.18	0.11	0.25	0.28
Vessel diameter (cm)	0.54	0.2	0.54	0.12	0.96
Mean curvature (1/cm)	2.03	0.53	1.67	0.26	**0.006**
Aneurysm volume (cm^3)	1.12	0.77	2.28	1.09	**0.003**
Aneurysm area (cm^2)	7.39	3.64	10.84	3.37	**0.008**

OSI, oscillatory shear index, POD, proper orthogonal decomposition; WSS, wall shear stress.

RESULTS

Stable versus unstable aneurysms: baseline characteristics

A total of 37 aneurysms were included in the study. All lesions involved the basilar artery. There were no vertebral artery lesions. Twenty-four aneurysms (64.5%) were stable over a mean of 40.8 months of follow-up and 13 aneurysms (35.2%) grew or ruptured over a mean of 51.9 months of follow-up. Mean aneurysm maximum diameter was larger in the unstable group than in the stable group (11.9±5.0 mm vs 7.6±1.8 mm, P=0.01). Aneurysms in the unstable group were more likely to have a fusiform or transitional morphology than those in the stable group (84.6% vs 45.8%, P=0.04). Aneurysms in the unstable group were more likely to be Mizutani type 3 than those in the stable group (54.2% vs 15.4%, P=0.035). Mean patient age in the stable and unstable groups were 60.6±13.6 and 58.8±15.7 years, respectively (P=0.74). Patients in the unstable group were more likely to smoke (61.5% vs 12.5%, P=0.002). There was no difference in sex distribution (P=0.41) or hypertension status (P=0.24). Sixteen aneurysms (43.2%) had intramural T1 hyperintensity and there was no difference in the prevalence of this finding between groups (P=0.12). The data are summarized in table 1.

Stable versus unstable aneurysms: hemodynamic outcomes

A summary of the hemodynamic characteristics of the stable and unstable aneurysms is provided in table 2. When compared with stable aneurysms, unstable aneurysms had lower shear rates (84.89/s (±87.07) vs 153.19/s (±118.91), P=0.05), lower velocities (9.3 cm/s (±6.79) vs 15.01 cm/s (±7.74), P=0.03), and lower vorticity (120.11/s (±122.71) vs 219.76/s (±170.65), P=0.049). Unstable aneurysms had higher mean oscillatory shear index (0.04±0.02 vs 0.01±0.01, P=0.001) and higher maximum oscillatory shear index (0.46±0.03 vs 0.40±0.11, P=0.02). Unstable aneurysms also had higher flow complexity (11.67 cm (±10.53) vs 4.32 cm (±5.01), P=0.03) and higher instability, as measured by proper orthogonal decomposition entropy (0.24±0.11 vs 0.11±0.07, P=0.001). Unstable aneurysms were larger (higher volume, P=0.003 and surface area, P=0.008) with lower surface curvature (mean curvature, P=0.006) than stable aneurysms. Examples of stable and unstable aneurysms illustrating these general hemodynamic differences are presented in figures 1 and 2, respectively.

Qualitatively, compared with stable cases, the unstable cases have regions of low wall shear stress and low flow velocity, co-located with focal aneurysmal dilatations of the vessel wall and regions of elevated wall shear stress where the inflow jets impact on the wall. Localized regions of high OSI are all observed in the regions of low wall shear stress. Additionally, flow patterns in the unstable cases are more complex, as illustrated by several vortex core line structures within those dilated regions. In the stable cases, strong swirling flows induced by the tortuous geometry of the vessels are observed (figures 1 and 2).

Non-stroke associated versus stroke associated aneurysms: baseline characteristics

Thirty aneurysms (81.1%) were not associated with stroke over a mean of 37.0 months of follow-up and seven aneurysms (18.9%) were associated with stroke over a mean of 77.0 months of follow-up. Mean aneurysm maximum diameter was larger in the non-stroke group than in the stroke group (9.5±4.1 mm vs 7.5±1.3 mm, P=0.03). There was no difference in aneurysm morphology between groups using both the Flemming (P=0.97) and Mizutani categorizations (P=1.00). Mean patient age in the non-stroke and stroke groups were 61.1±13.5 and

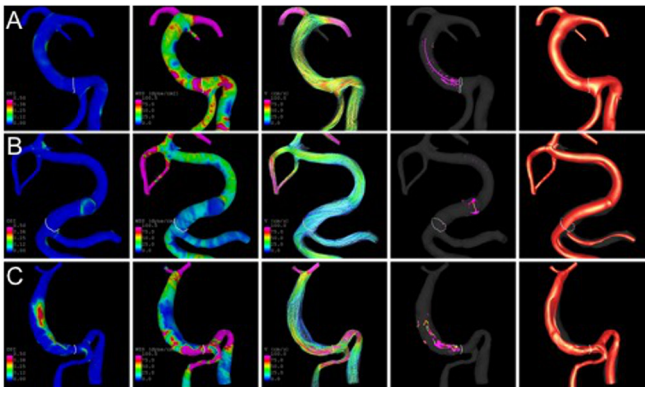

Figure 1 Flow visualization at peak systole in three examples of stable cases. Left to right: oscillatory shear index (OSI), wall shear stress, flow streamlines, vortex core lines, and iso-velocity surface (30 cm/s). (A) Dolichoectatic aneurysm with a maximum cross sectional diameter of 8 mm. Note the uniformly low OSI, relatively high wall shear stress, and uniform flow streamlines and flow velocity. (B) Dolichoectatic lesion with a focal area of aneurysmal dilatation, consistent with a transitional morphology. Note that in the region of the focal dilatation there is increased OSI, low wall shear stress, and complex vortices. The rest of the lesion has uniformly low OSI, high wall shear stress, and uniform flow. (C) Dolichoectatic lesion with a maximum diameter of 9 mm. In the mid-section of the basilar artery there is focally high OSI, low wall shear stress, and slow flow. The rest of the lesion has uniformly low OSI, high wall shear stress, and homogeneous flow.

55.1±17.3 years, respectively (P=0.42). There was no difference in sex distribution (P=0.12) or hypertension status (P=0.39). The data are summarized in table 3.

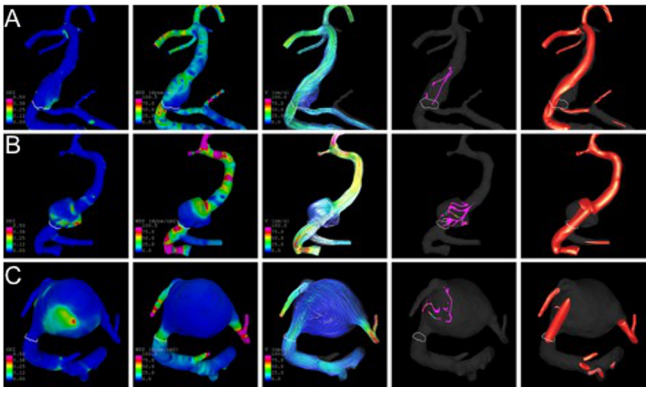

Figure 2 Flow visualization at peak systole in three examples of unstable cases. Left to right: oscillatory shear index (OSI), wall shear stress, flow streamlines, vortex core lines, and iso-velocity surface (30 cm/s). (A) A smaller transitional type aneurysm with a focal dilatation of the basilar trunk of 10 mm. Note that in this focal dilatation there is elevated OSI, low wall shear stress, and slow flow. This region grew on follow-up imaging. (B) Transitional type aneurysm with tortuosity of the entire basilar artery and a focal dilatation at the basilar trunk. Note the elevated OSI, low wall shear stress in the region of the basilar trunk, complex vortices, and slow flow. This lesion ruptured on follow-up. (C) Complex basilar trunk lesion aneurysm which is superimposed on an already tortuous and dolichoectatic basilar artery. Note the high OSI in the aneurysm sac, the uniformly low wall shear stress, and the slow velocity and complex vortices. This lesion presented with a perforator infarct and ruptured just 2 weeks after presentation.

Table 3 Baseline characteristics of the non-stroke and stroke groups

	No stroke	Stroke	P value
No (%) of patients	30 (81.1)	7 (18.9)	–
Age (years) (mean (SD))	61.1 (13.5)	55.1 (17.3)	0.42
Men (n (%))	22 (73.3)	7 (100.0)	0.12
Follow-up (months) (mean (SD))	37.0 (40.1)	77.7 (74.0)	0.21
Aneurysm type (n (%))			
Fusiform	8 (26.7)	2 (28.6)	
Dolichoectatic	12 (40.0)	3 (42.9)	
Transitional	10 (33.3)	2 (28.6)	0.97
Mizutani type			
Type 2	12 (40.0)	3 (42.9)	1.00
Type 3	18 (60.0)	4 (57.1)	
Mural T1 hyperintensity (n (%))	13 (44.8)	3 (42.9)	0.93
Maximum diameter (mm) (mean (SD))	9.5 (4.1)	7.5 (1.3)	0.03
Comorbidities			
CAD	10 (33.3)	3 (42.9)	0.63
PAD	0 (0.0)	0 (0.0)	1
Hypertension	21 (70.0)	6 (85.7)	0.39
Diabetes mellitus	4 (13.3)	1 (14.3)	0.95
Hyperlipidemia	18 (60.0)	5 (71.4)	0.57
Tobacco use	9 (30.0)	2 (28.6)	0.99

CAD, coronary artery disease; PAD, peripheral artery disease.

Non-stroke associated versus stroke associated aneurysms: hemodynamic outcomes

There were no significant differences in any of the hemodynamic outcomes between the no stroke and stroke groups (table 4). Shear rates (P=0.31), velocities (P=0.24), vorticity (P=0.32), and maximum oscillatory shear index (P=0.51) were similar between groups.

DISCUSSION

Our CFD study of 37 VBDAs with longitudinal follow-up found significant differences in the hemodynamics of unstable versus stable lesions and no differences in the hemodynamic characteristics of lesions in the no stroke and stroke groups. Unstable aneurysms generally had lower flow conditions with lower velocities, vorticities, and shear rates. In addition, they had more oscillatory flow patterns, more complex flow patterns, and higher proper orthogonal decomposition entropy, factors indicative of more unstable flow. These findings are important as they suggest that CFD might provide mechanistic information regarding hemodynamic factors that result in growth or rupture of these complex lesions. It is important to point out that factors such as aneurysm size and morphology likely confounded our results, thus highlighting the need to confirm our results with larger studies with a single a priori hypothesis.

No longitudinal studies examining the hemodynamic characteristics of VBDAs have been published to date. However, there have been several case reports examining the hemodynamic characteristics of VBDAs. In a case report of one patient with vertebrobasilar dolichoectasia, Han *et al* noted complex flow in the distal aspect of the basilar artery with areas of low wall shear stress at the vertebrobasilar junction and inferior segment of the basilar artery.[19] These are typically the areas where focal fusiform dilatations occur in VBDAs. In a case report examining hemodynamic characteristics of a giant vertebrobasilar junction aneurysm, Graziano *et al* found high velocity of blood flow at

Table 4 Hemodynamic outcomes of the stroke and non-stroke groups

	No stroke		Stroke		
Variable	**Mean**	**SD**	**Mean**	**SD**	**P value**
Hemodynamics					
Kinetic energy (erg)	348.39	437.58	482.11	464.08	0.51
Shear rate (1/s)	172.04	119.1	119.2	110.57	0.31
Velocity (cm/s)	15.56	5.54	12.41	8.23	0.24
Vorticity (1/s)	245.49	170.9	170.58	158.35	0.32
Viscous dissipation (erg)	1001.26	1593.39	531.15	951.81	0.48
WSSmax (dyn/cm^2)	269.09	256.94	148.19	144.44	0.27
WSSmin (dyn/cm^2)	0.03	0.02	0.09	0.34	0.39
WSSmean (dyn/cm^2)	21.28	17.04	14.16	13.3	0.33
OSImax	0.39	0.13	0.43	0.09	0.51
OSImean	0.02	0.01	0.03	0.02	0.14
Core line length/flow complexity (cm)	10.25	8.03	6.12	8.05	0.25
POD entropy/flow stability	0.15	0.07	0.15	0.11	0.89
POD num/flow stability	1	0	1.13	0.43	0.1
Maximum velocity (cm/s)	132.36	115.59	76.22	61.79	0.25
Mean maximum velocity (cm/s)	76.03	65.06	44.09	35.94	0.25
Geometry					
Gaussian curvature	0.05	0.19	0.05	0.21	0.94
Vessel diameter (cm)	0.53	0.18	0.54	0.18	0.89
Mean curvature (1/cm)	1.97	0.38	1.89	0.5	0.62
Aneurysm volume (cm^3)	1.25	0.86	1.59	1.09	0.38
Aneurysm area (cm^2)	8.12	3.82	8.72	3.95	0.72

OSI, oscillatory shear index; POD, proper orthogonal decomposition; WSS, wall shear stress.

the aneurysm neck with stagnant, low flow conditions in the central portion of the aneurysm.[20] In another case report, Hassan *et al* reported CFD findings in a patient with a giant fusiform vertebrobasilar aneurysm and found complex intra-aneurysmal flow patterns with vortex type flow in an area of thrombosis.[21] Overall, these findings are similar to ours which demonstrated low flow conditions, including low wall shear stress and complex flow patterns related to VBDAs.

Several studies in the saccular aneurysm literature have pointed to wall shear stress conditions being associated with aneurysm formation and instability.[9 22–26] In our study, we found that low wall shear stress conditions were associated with aneurysm progression. There are a number of mechanisms proposed to explain why low wall shear stress conditions could precipitate aneurysm progression. Endothelial cells depend on a certain level of wall shear stress to be viable. However, endothelial cells which are exposed to low wall shear stress conditions are associated with an elevated oxidative state, have increased apoptosis, and have increased cell turnover.[27–32] Low wall shear stress is also associated with alterations in gene expression patterns which promote proinflammatory signal pathways.[27–32] Furthermore, differences in the hemodynamic environments of stable and unstable aneurysms could result in degeneration of the tunica intima, a factor which has been associated with the pathogenesis of VBDAs.

Vorticity and flow complexity were also associated with aneurysm instability in our study. Prior studies in the saccular aneurysm literature have found that multiple smaller vortices and complex flow patterns are associated with aneurysm instability.[26 33] In a longitudinal case control study of 24 aneurysms, our group found that the mean aneurysm vorticity was about half as small in unstable aneurysms compared with stable aneurysms.[9] In general, the simple stable flow patterns seen in stable aneurysms are associated with a large vortex whereas the complex unstable flow patterns in unstable growing and ruptured aneurysms are more likely to result in multiple smaller vortices. Presumably, complex flow patterns (ie, multiple smaller vortices) can increase aneurysm wall permeability, for example via altered oxygen transport to the wall, thus promoting inflammatory cell infiltration and favoring intra-aneurysmal thrombus formation. This is particularly interesting given the fact that intra-aneurysmal thrombus has been shown to be a risk factor for growth and rupture of VBDAs.[4 5]

Our study also has potential immediate clinical implications. While CFD is not currently integrated into clinical practice, some of the CFD parameters described in this study have useful correlates on conventional imaging. Slow and complex flow, which were shown to be correlated with aneurysm instability in our study, are identifiable on three-dimensional time of flight MRA by the presence of signal loss or turbulence in the aneurysm sac. Areas of low wall shear stress and slow flow can be identified on conventional angiography by the presence of stasis in the aneurysmal vessel. High intra-aneurysmal luminal signal on T2 and T1 weighted images are also indicators of turbulent flow. From a practical standpoint, the findings from our study suggest that imaging evidence of slow or turbulent flow could potentially be associated with a poorer prognosis for the aneurysm in addition to conventional risk factors, such as size, location, and the presence of intramural hematoma.

Limitations

Our study has limitations. Given the minimum follow-up time of 12 months to confirm aneurysm stability, it is possible that very slowly growing aneurysms were included in the stable group. Our study was a small study and is thus likely to be underpowered to detect smaller differences in various hemodynamic parameters in both our aneurysm stability analysis and in our stroke analysis. We did not correct for multiple comparisons in this study due to its exploratory nature.

We could not perform a multivariate analysis to determine if CFD parameters were independently associated with poor outcomes due to the small number of events. There were important baseline differences between groups in terms of aneurysm size and morphology so it is difficult to determine if these variables confounded our CFD findings. There are also limitations related to CFD models. CFD models assume rigid aneurysm walls, normal physiologic conditions, and Newtonian flow.[34] Flow instabilities may be masked by the coarse temporal resolution of the simulations. While the solver has been verified and validated against angiographic observations, such data are certainly not ground in truth. Aneurysm inlets were manually delineated on the reconstructed models. The conclusions of this paper are based on CFD results which are certainly not ground in truth.

Another limitation of this study is the fact that we used the Flemming criteria for assessing aneurysm morphology. There are a number of criteria available for assessment of aneurysm morphology including, notably, the Mizutani criteria which have a strong correlation with aneurysmal pathologic characteristics.[35] Data from our study suggest a correlation between abnormal aneurysm hemodynamics and progression, but by no means should these findings be considered causative. It is important for readers to cautiously consider these findings until they are confirmed by larger studies with a single a priori hypothesis.

CONCLUSIONS

This small exploratory longitudinal study suggests there may be hemodynamic differences between unstable and stable VBDAs. Unstable VBDAs appear to be under lower flow conditions with lower velocity, vorticity, and shear rates, and have more oscillatory flow, findings that have also been reported in the saccular aneurysm literature. There was no difference in hemodynamic characteristics of aneurysms in the stroke and no stroke groups. Larger multi-institutional collaborative studies may be helpful to better define the relationship between VBDA hemodynamics and risk of aneurysm instability and stroke.

Contributors All authors made (1) substantial contributions to conception or design of the work or the acquisition, analysis, or interpretation of data for the work; (2) drafting of the work or revising it critically for important intellectual content; (3) final approval of the version to be published; and (4) are in agreement to be accountable for all aspects of the work in ensuring that questions related to the accuracy or integrity of any part of the work are appropriately investigated and resolved.

Funding This research received no specific grant from any funding agency in the public, commercial, or not-for-profit sectors.

Competing interests WB: CEO of Marblehead Medical LLC and patents pending in balloon catheter technologies; consultant for Johnson and Johnson. DFK: President of Marblehead Medical LLC and patents pending in balloon catheter technologies.

Ethics approval The study was approved by the Mayo Clinic institutional review board.

Provenance and peer review Not commissioned; externally peer reviewed.

Data sharing statement Data could be made available by contacting the corresponding author via email.

REFERENCES

1 Shapiro M, Becske T, Riina HA, *et al*. Non-saccular vertebrobasilar aneurysms and dolichoectasia: a systematic literature review. *J Neurointerv Surg* 2014;6:389–93.
2 Pico F, Labreuche J, Amarenco P. Pathophysiology, presentation, prognosis, and management of intracranial arterial dolichoectasia. *Lancet Neurol* 2015;14:833–45.
3 Saliou G, Sacho RH, Power S, *et al*. Natural history and management of basilar trunk artery aneurysms. *Stroke* 2015;46:948–53.
4 Nasr DM, Brinjikji W, Rouchaud A, *et al*. Imaging characteristics of growing and ruptured vertebrobasilar non-saccular and dolichoectatic aneurysms. *Stroke* 2016;47:106–12.
5 Flemming KD, Wiebers DO, Brown RD, *et al*. The natural history of radiographically defined vertebrobasilar nonsaccular intracranial aneurysms. *Cerebrovasc Dis* 2005;20:270–9.
6 Flemming KD, Wiebers DO, Brown RD, *et al*. Prospective risk of hemorrhage in patients with vertebrobasilar nonsaccular intracranial aneurysm. *J Neurosurg* 2004;101:82–7.
7 Cebral JR, Mut F, Weir J, *et al*. Association of hemodynamic characteristics and cerebral aneurysm rupture. *AJNR Am J Neuroradiol* 2011;32:264–70.
8 Cebral JR, Vazquez M, Sforza DM, *et al*. Analysis of hemodynamics and wall mechanics at sites of cerebral aneurysm rupture. *J Neurointerv Surg* 2015;7:530–6.
9 Brinjikji W, Chung BJ, Jimenez C, *et al*. Hemodynamic differences between unstable and stable unruptured aneurysms independent of size and location: a pilot study. *J Neurointerv Surg* 2017;9:376–80.
10 Cebral JR, Castro MA, Appanaboyina S, *et al*. Efficient pipeline for image-based patient-specific analysis of cerebral aneurysm hemodynamics: technique and sensitivity. *IEEE Trans Med Imaging* 2005;24:457–67.
11 Castro MA, Putman CM, Cebral JR. Computational fluid dynamics modeling of intracranial aneurysms: effects of parent artery segmentation on intra-aneurysmal hemodynamics. *AJNR Am J Neuroradiol* 2006;27:1703–9.
12 Raschi M, Mut F, Byrne G, *et al*. CFD and PIV analysis of hemodynamics in a growing intracranial aneurysm. *Int J Numer Method Biomed Eng* 2012;28:214–28.
13 Cebral JR, Pergolizzi RS, Putman CM. Computational fluid dynamics modeling of intracranial aneurysms: qualitative comparison with cerebral angiography. *Acad Radiol* 2007;14:804–13.
14 Ford MD, Alperin N, Lee SH, *et al*. Characterization of volumetric flow rate waveforms in the normal internal carotid and vertebral arteries. *Physiol Meas* 2005;26:477–88.
15 Cebral JR, Castro MA, Putman CM, *et al*. Flow-area relationship in internal carotid and vertebral arteries. *Physiol Meas* 2008;29:585–94.
16 Murray CD. The physiological principle of minimum work applied to the angle of branching of arteries. *J Gen Physiol* 1926;9:835–41.
17 Mut F, Löhner R, Chien A, *et al*. Computational hemodynamics framework for the analysis of cerebral aneurysms. *Int J Numer Method Biomed Eng* 2011;27:822–39.
18 Byrne G, Mut F, Cebral J. Quantifying the large-scale hemodynamics of intracranial aneurysms. *AJNR Am J Neuroradiol* 2014;35:333–8.
19 Han JT, Qiao HT, Han X, *et al*. [Analysis of vertebrobasilar dolichoectasia based on computational fluid dynamics]. *Beijing Da Xue Xue Bao Yi Xue Ban* 2015;47:302–4.
20 Graziano F, Russo VM, Wang W, *et al*. 3D computational fluid dynamics of a treated vertebrobasilar giant aneurysm: a multistage analysis. *AJNR Am J Neuroradiol* 2013;34:1387–94.
21 Hassan T, Ezura M, Timofeev EV, *et al*. Computational simulation of therapeutic parent artery occlusion to treat giant vertebrobasilar aneurysm. *AJNR Am J Neuroradiol* 2004;25:63–8.
22 Sforza DM, Kono K, Tateshima S, *et al*. Hemodynamics in growing and stable cerebral aneurysms. *J Neurointerv Surg* 2016;8:407–12.
23 Miura Y, Ishida F, Umeda Y, *et al*. Low wall shear stress is independently associated with the rupture status of middle cerebral artery aneurysms. *Stroke* 2013;44:519–21.
24 Can A, Du R. Association of hemodynamic factors with intracranial aneurysm formation and rupture: systematic review and meta-analysis. *Neurosurgery* 2015.
25 Boussel L, Rayz V, McCulloch C, *et al*. Aneurysm growth occurs at region of low wall shear stress: patient-specific correlation of hemodynamics and growth in a longitudinal study. *Stroke* 2008;39:2997–3002.
26 Xiang J, Natarajan SK, Tremmel M, *et al*. Hemodynamic-morphologic discriminants for intracranial aneurysm rupture. *Stroke* 2011;42:144–52.
27 Doenitz C, Schebesch KM, Zoephel R, *et al*. A mechanism for the rapid development of intracranial aneurysms: a case study. *Neurosurgery* 2010;67:1213–21.
28 Lu G, Huang L, Zhang XL, *et al*. Influence of hemodynamic factors on rupture of intracranial aneurysms: patient-specific 3D mirror aneurysms model computational fluid dynamics simulation. *Am J Neuroradiol* 2011;32:1255–61.
29 Kraiss LW, Geary RL, Mattsson EJR, *et al*. Acute reductions in blood flow and shear stress induce platelet-derived growth factor-a expression in baboon prosthetic grafts. *Circ Res* 1996;79:45–53.
30 Cho A, Mitchell L, Koopmans D, *et al*. Effects of changes in blood flow rate on cell death and cell proliferation in carotid arteries of immature rabbits. *Circ Res* 1997;81:328–37.
31 Chiu J-J, Chen C-N, Lee P-L, *et al*. Analysis of the effect of disturbed flow on monocytic adhesion to endothelial cells. *J Biomech* 2003;36:1883–95.
32 Malek AM, Alper SL, Izumo S. Hemodynamic shear stress and its role in atherosclerosis. *JAMA* 1999;282:2035–42.
33 Cebral JR, Castro MA, Burgess JE, *et al*. Characterization of cerebral aneurysms for assessing risk of rupture by using patient-specific computational hemodynamics models. *AJNR Am J Neuroradiol* 2005;26:2550–9.
34 Kallmes DF. Point: CFD-computational fluid dynamics or confounding factor dissemination. *Am J Neuroradiol* 2012;33:395–6.
35 Mizutani T, Miki Y, Kojima H, *et al*. Proposed classification of nonatherosclerotic cerebral fusiform and dissecting aneurysms. *Neurosurgery* 1999;45:253–9.